Problems Caused by Ion Sputtering for the Mesh-Replica Method and Caution in Measuring Sputtered Surface Profiles

M. Suzuki*, M. Kaise[1], T. Kimura[1], and S. Tanuma[1]

ULVAC-PHI, Inc., 370 Enzo, Chigasaki, Kanagawa 253-8522, Japan

[1]*National Institute for Materials Science, 1-2-1 Sengen, Tsukuba, Ibaraki 305-0047, Japan*

*msuzuki@phi.com

Received 3 October 2004; Accepted 11 January 2005

The Mesh-Replica Method has been proposed to estimate a sputtering rate of an actual material instead of that of a reference calibration material because this method is easy and convenient. It, however, involves several problems such as (1) a mesh sliding with the specimen assemble wrapped with aluminum foil, (2) formation of a micro-trench at the side of the crater bottom, (3) generation of an artificial profile of sputtered surface mainly due to image processing in AFM (atomic force microscopy) measurements, and (4) leveling difficulty of line profiling with a stylus profilometer because of insufficient retrained areas. In this paper, these examples are demonstrated using proximity observation techniques. In order to solve these problems, we examined the Mesh-Replica Method using an isolated aperture in a thin metal plate, resulting in good stylus profiles with less effort. Finally we propose an asymmetric assortment of apertures that is useful for stylus measurements and assignment of the incident direction of ion beam.

INTRODUCTION

Depth profiling [1] is one of the key technologies to characterize atomic concentration in depth using AES (Auger electron spectroscopy), XPS (x-ray photoelectron spectroscopy), and SIMS (secondary ion mass spectrometry). In depth profiles, the abscissa and ordinate are usually expressed by the sputtering time and intensity (or concentration), respectively. The sputtering time is usually converted to the sputtered depth in practical depth profiling analysis, multiplying it by the sputtering rate for the analyzed material [2]. It is, however, not easy to know the actual sputtering rate of a respective material and the sputtering rate obtained from a reference calibration sample is applied instead of an actual one. The "Mesh-Replica Method" was proposed to experimentally measure the sputtering rate of homogeneous materials by using a metallic mesh [3] over the sample to be sputtered and it is the subject of a future standard with the International Standard Organization, TC (Technical Committee) 201 on Surface Chemical Analysis, SC (Sub-Committee) 4 on Depth Profiling. This Mesh-Replica Method has been applied to measure relative sputtering rates of many materials against the silicon dioxide film as the reference material, such as GaAs [4], silicon [5], and aluminum oxide [6]. The SERD (sputter etching rate detabase) project in SASJ (Surface Analysis Society of Japan) is building a database of relative sputtering rates to that of the standard sample of silicon thermal dioxide films, and offering them on their web site [7]. The size of mesh opening was also investigated in the Mesh-Replica Method [8].

In this paper we will demonstrate an example of failure of the Mesh-Replica Method and will report results obtained by proximity techniques and stylus profilometer for sputtered replica patterns. We would finally like to call users' attention and propose a better mask with hole than a mesh.

EXPERIMENTAL

The specimens used were cut from a Si(100) wafer with a thermally oxidized 100-nm-thick SiO_2 film. The meshes were commercial ones made from copper and meshes were mounted on the specimen,

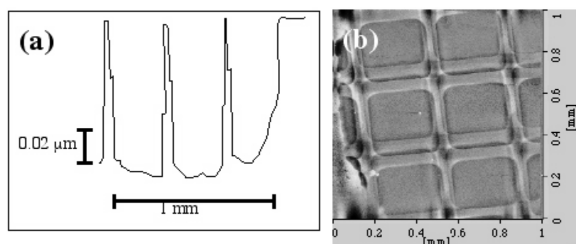

Fig. 1: Stylus profile (a) and AFM image (b) for the replica pattern in which the 75-mesh grid slid during ion sputtering. There is a step-wise structure on the sides of the wall retained by the mesh grid in (a). The double replica pattern is seen in the AFM image (b).

wrapping with aluminum foils with circular holes, according to the previous reported procedure [3]. The isolated apertures (50, 100, and 200 μm in diameter, 2 mm apart from each other) in a 10 μm-thick Mo plate (about 7 x 10 mm^2) were also prepared and it was placed on the specimen by spring pins. The sputtering procedures were performed with the AES apparatus (PHI-680) and the primary ion was Ar^+ with the acceleration energy of 2 keV hit the specimen surfaces with the incident angle of 30 degrees from the surface normal. The ion beam was raster-scanned for 1 x 1 mm^2 and the sputtering was stopped in the region of the oxide layer less than 100 nm. The replica patterns were measured by proximity techniques of the stylus profilometer (surfcom 900A from TOKYO SEIMITSU) and atomic force microscopes (Nanopics 2100 from SII and XE-150 from PSIA) as well as SE (secondary electron) images in the AES apparatus.

RESULTS AND DISCUSSIONS

Figure 1 shows an example of failure, where the 75-mesh slid between the specimen and an aluminum foil during ion sputtering. A part of cross-sectional profile measured by the stylus profilometer and an AFM top view image are shown as Fig. 1(a) and 1(b), respectively. We are guessing that the mesh slid along the vertical direction in Fig. 1(b), resulting in the vertical doublet-pattern. The width of mesh-bar is 50μm and it almost corresponds to the sliding distance. The cross-sectional profile was shown in Fig. 1(a) when the stylus probe was scanned along the direction corresponding the sliding direction. It is found that there is a vertical step-wise structure at the

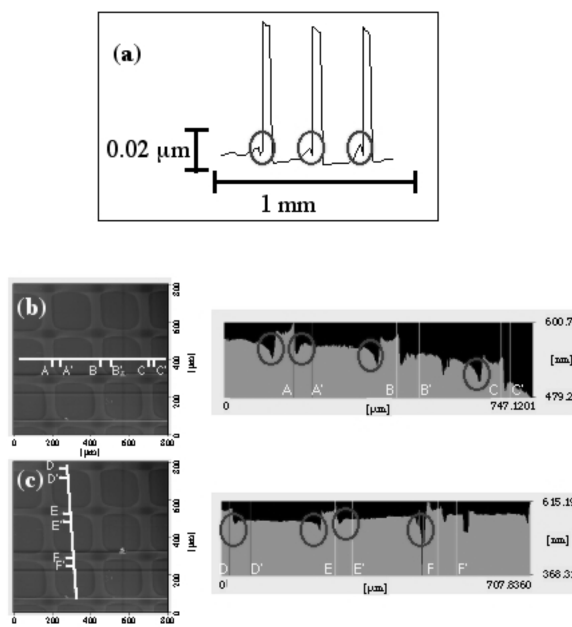

Fig. 2: (a) Cross-sectional stylus profile for the 100-mesh replica pattern. There is a micro-trench structure in the circles. (b) AFM top view and the cross-sectional profile along the horizontal line in the top view. (c) AFM top view and the cross-sectional profile along the vertical line in the top view.

both sides of the wall corresponding the position, where the original surface is retained from ion sputtering by the grid bar. The bottom shape is also undulating in the stylus profile. When the stylus probe was scanned along the horizontal direction in Fig. 1(b), there was not a doublet structure in a profile. In the latter case, one may measure the sputtered depth without the notice of this sliding problem. Even in the scanning along the sliding direction, one might not care about an uncertain profile if he/she does not observe the surface morphology with two-dimensional method such as an SEM or AFM. Furthermore, we have to learn a most important thing that it is needed to make a tight mechanical contact of a specimen, mesh and aluminum foil.

The replica patterns formed with the 100-mesh are shown in Fig. 2. A small ditch structure is shown at the right side corner of the bottom in the stylus profile of Fig. 2(a). Though this feature is not observed at the left corners, it is thought to be a micro-trenching structure due to the reflected ions, corresponding the mechanism reported for the plasma process for LSI pattern fabrication [9]. AFM images

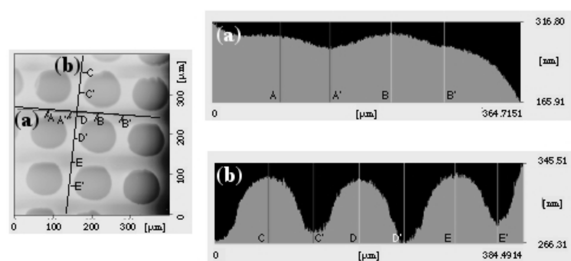

Fig. 3: AFM top view image of the 200-mesh replica pattern, cross-sectional profile along the line (a) on the mesh grid part, and that along the line (b). The image was image-processed to be flattened.

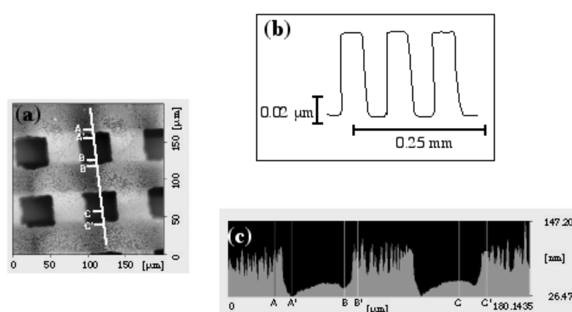

Fig. 4: (a) AFM top view image of the 300-mesh replica pattern. (b) Cross-sectional stylus profile. (c) Cross-sectional profile along the line in the AFM top view.

and the cross-sectional profiles along the lines in the top view images are shown in Fig. 2(b) and 2(c). The AFM images were image-processed so as to flatten and level the sputtered bottom surfaces through mesh openings. The micro-trenches exist at both corners of the sputtered crater bottoms and make a partial convex shape in both directions (see Figs. 2(b) and 2(c)). We have to take care to measure a position without the micro-trenching areas. It is important that results by both methods correlate with one another. Two main problems are (1) whether a micro-trenching structure exists at one side in Fig. 2(a) or at both sides in Figs. 2(b) and 2(c), and (2) a micro-trench is formed between a grid-wall and protrusion feature such like in Fig. 2(a) or it is a smooth structure in Figs. 2(b) and 2(c). We should also pay attention to the image processing technique for the AFM data analysis to reduce distortion caused by the measurement conditions. Optimized measurement conditions for the stylus profilometer and AFM to get consistent results should be investigated.

The AFM images from the replica pattern of the 200-mesh are shown in Fig. 3. Shown here are the cross-sectional profiles on the retained mesh grid parts corresponding to orthogonal directions of (a) and (b). The profiles should be generally flat since these parts were hidden by the mesh grid from energetic ions. The waviness is about 20 nm for the direction (a), but about 50 nm for the direction (b). This artifact failure was confirmed by the fact that the direction of the corrugation did not change even when the specimen was rotated by 90 degrees on the specimen stage, though it is not shown here. This is an artifact from inappropriate image processing that was performed in order to flatten the raw image with a tilt distortion caused by the three-dimensional cross-talk movement in the AFM scanner. When we scan the sample to measure the depth, an image processing is generally employed to make a clear image. We do not know the metrological traceability of accuracy using our image processing software, though the problems in Fig. 3 may be solved after the data is fairly processed.

The case of the 300-mesh replica pattern is shown in Fig. 4. In the AFM top view image (Fig. 4 (a)), the same problem shown in Fig. 3 takes place. The micro-trench seems to exist in the cross-sectional profile in Fig. 4(c) of the AFM data, though the stylus cross-sectional profile looks good with no artifacts in Fig. 4(b). The same specimen was observed with a cross-talk free AFM instrument (XE-150) as shown in Fig. 5. Figure 5(a) shows an OM (optical microscope) image with AFM and the upper-left corner out of the mesh opening has a different contrast from other grid areas. When the specimen was rotated by 90 degrees, this feature was also rotated, judging it true. The composed AFM images (Fig. 5(b)) correspond to the areas of two squares in Fig. 5(a), which are in piles of raw data without any image processing. From the AFM image it is found that the upper-left area out of the hole is higher than the other retained area by the mesh grid. These higher areas might be formed by the materials sputtered from the substrate or the mesh. The cross-sectional profiles, corresponding the three lines “R”, “G”, and “B”, are shown in Fig. 5(c). The cross-sectional shapes of the sputtered bottom surface are flat, and there is not a micro-trench that is artificially shown in

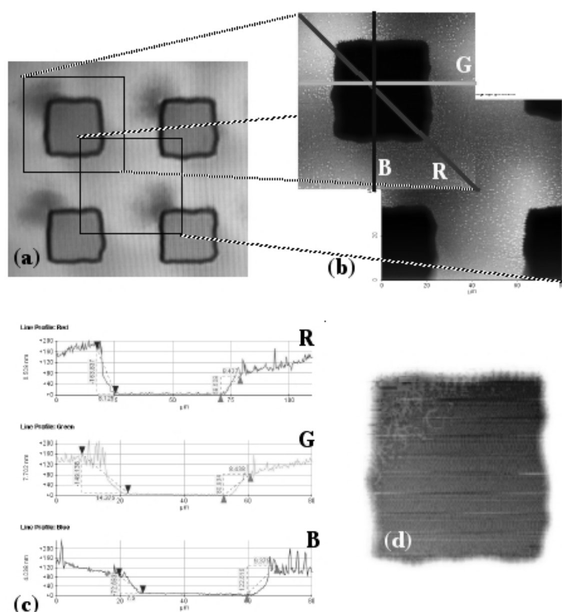

Fig. 5: (a) OM image of the 300-mesh replica pattern. (b) AFM top views corresponding to square areas in the OM image. (c) Cross-sectional profiles along the three lines in (b). (d) AFM image of the sputtered bottom area.

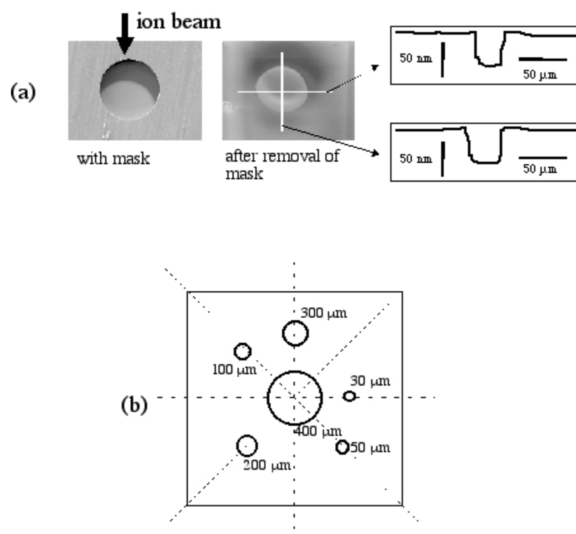

Fig. 6: (a) Sputtering process with an isolated aperture and SEM image after removal of the mask and cross-sectional stylus profiles along the orthogonal lines traveling the circular sputtered area. (b) An example of proposal of asymmetric assortment of apertures.

Fig. 4. Figure 5(d) shows a fine morphology of the bottom surface and there is a textile-like structure in the upper-left corner inthis bottom. It is thought that this feature correlates with the upper-left higher area out of the sputtered area. The height of the textile structure is so small that the measured sputtered depth is not affected. It is, furthermore, needed to study the formation mechanism of a set of higher corrugation and textile feature in the Mesh-Replica Method.

SUMMARY AND PROPOSAL

In the Mesh-Replica Method, there are merits that (1) the cost of materials (TEM compatible mesh and aluminum foil) is reasonable and (2) the setup method of the specimen, mesh, and aluminum foil is very easy. As mentioned in the previous chapter, however, it involves problems that a specimen slides in the aluminum wrapping assembly or the interference of adjacent mesh openings takes place. For measuring the sputtered depth, it is difficult to align the traveling direction of the stylus probe with the mesh orientation and to optimize the leveling of the stylus profilometer trace when the retained original surface is too small. It is also important to align the ion beam axis with the grid mesh.

In order to solve the former problems, we examined the Mesh-Replica Method using an isolated aperture since it offers the advantage of a larger un-sputtered surface. An example is shown in Fig. 6(a) for the 50 µm aperture. A distorted replica pattern is seen since there was not good contact between the specimen and aperture. The stylus profiles, however, give us enough information of the sputtered depth in any orientation to the ion beam direction. It was also very easy to level the profilometer and measure the crater depth. We also obtained good results for 100 and 200 µm apertures.

We propose a special assortment (assumedly 5 x 5 mm^2) of apertures as shown in Fig. 6(b). The largest central aperture is convenient for sputtering with sample rotation, though it is not described in this report. Several apertures of 30 to 300 µm are arranged with sufficient separation distances making it useful for leveling using a stylus profilometer. Since the aperture configuration is asymmetric, that makes it easy to align the ion beam incidence direction using an SEM image. We will evaluate this proposal in future SASJ activities, and hopefully will prepare it as a standard mesh to estimate ion-sputtering rates.

ACKNOWLEDGMENTS

The authors thank Dr. Sang-il Park and Mr. Petric Yoon, PSIA, for their help to measure the replica pattern using the cross-talk free AFM instrument. They also wish to thank Dr. Isao Nakatani, NIMS, for his helpful suggestions.

REFERENCES

[1] ISO/TR 15969:2001, Surface chemical analysis -- Depth profiling -- Measurement of sputtered depth.

[2] ISO 14606:2000, Surface chemical analysis -- Sputter depth profiling -- Optimization using layered systems as reference materials.

[3] M. Suzuki, K. Mogi, and H. Ando, J. Surf. Anal. **5**, 188 (1999).

[4] M. Inoue, J. Korean Vacuum Soc. **9**, 103 (2000).

[5] K. Mogi, T. Ogiwara, and M. Suzuki, J. Surf. Anal. **9**, 514 (2002).

[6] S. Araki, H. Tohma, and SERD Project of SASJ, J. Surf. Anal. **9**, 451 (2002).

[7] http://serd.sasj.jp/

[8] M. Suzuki, K. Mogi, and T. Ogiwara, J. Surf. Anal. **10**, 144 (2003).

[9] “Topography Evolution During Semiconductor Processing” by T. S. Cale et al. in “Plasma Processing of Semiconductors” ed. by P. F. Williams, NATO ASI Series E336, Kluwer Academic Publishers, 1997.